

Determination of the Electron Transfer Number for the Oxygen Reduction Reaction: From Theory to Experiment

Ruifeng Zhou,^{†,‡,||} Yao Zheng,[†] Mietek Jaroniec,[§] and Shi-Zhang Qiao^{*,†}

[†]School of Chemical Engineering, The University of Adelaide, Adelaide, South Australia 5005, Australia

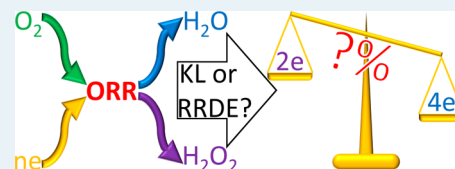
[‡]Australian Institute for Bioengineering and Nanotechnology, The University of Queensland, St Lucia, Queensland 4072, Australia

[§]Department of Chemistry and Biochemistry, Kent State University, Kent, Ohio 44242, United States

S Supporting Information

ABSTRACT: The forced convection methods on the rotating disk and ring-disk electrodes are carefully analyzed toward their use for calculation of the electron transfer number (n) for the oxygen reduction reaction (ORR) on various catalysts. It is shown that the widely used Koutecky–Levich (KL) method is not suitable to determine n for the ORR either theoretically or experimentally. From a theoretical viewpoint, the ORR is neither a single-step nor a one-way reaction and, therefore, does not fulfill the assumptions of the KL method. From an experimental viewpoint, n is significantly dependent on the angular velocity of the rotating disk electrode, contradicting the assumption of constant n in the KL theory. An improved model is used to establish the aforementioned relationship between n and angular velocity. The recommended way to determine n for the ORR in alkaline electrolytes is to use the rotating ring-disk electrode with a properly biased Au ring, supplemented by the calibration of the collection efficiency.

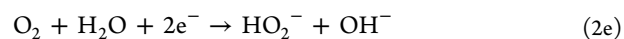
KEYWORDS: oxygen reduction reaction, electron transfer number, hydrogen peroxide production, rotating ring-disk electrode, Koutecky–Levich equation



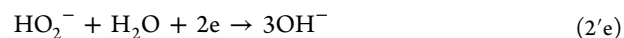
1. INTRODUCTION

1.1. Inconsistent Calculation of Electron Transfer Number. The electron transfer number (n) is one of the most important characteristics of the electrocatalytic oxygen reduction reaction (ORR) in aqueous electrolytes, which not only reflects the efficiency of oxygen conversion but also provides information on the ORR mechanism. In practice, low n leads to an inexpensive and safe way to produce H_2O_2 ,^{1–4} but high H_2O_2 concentration deteriorates the proton exchange membrane in fuel cells.^{5–7} With increasing interest in fuel cells, more and more researchers have adopted n as a key parameter to evaluate the performance of electrocatalysts.^{8–13} Conventionally, two experimental methods are widely used to determine n : i.e., the rotating ring-disk electrode (RRDE) method and the Koutecky–Levich (KL) method. However, these methods were developed over half a century ago, under the assumptions of elementary reactions.^{14–16} The applicability of these methods for the ORR has not been examined for a long time, especially in relation to the recently developed nanostructured and 3D catalysts in alkaline electrolytes. According to our and others' previous studies performed for a wide variety of electrocatalysts, the n value obtained by the RRDE (n_{RRDE}) and KL (n_{KL}) methods usually did not coincide.^{17–23} The KL plots are often not linear, and the n_{KL} values sometimes exceed theoretical limits. Thus, it is highly desirable to carefully re-examine the aforementioned methods from both theoretical and experimental viewpoints to figure out the problem and provide a general, correct, and accurate way to determine n .

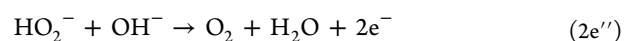
1.2. Basic Concept and Traditional Calculation Methods of n . During the ORR, an O_2 molecule can receive either two or four electrons to form H_2O_2 or H_2O (in the forms of HO_2^- and OH^- in alkaline electrolyte), via reactions 4e and 2e.



H_2O_2 can be further reduced to H_2O via



Reactions 4e, 2e, and 2'e are referred to as "subreactions" of the ORR in this manuscript. The combination of reactions 2e and 2'e gives the same outcome as reaction 4e. The difference in the direct and indirect pathways is whether free H_2O_2 molecules are released to the electrolyte. The n value is defined as the arithmetic mean of the number of electrons finally received by an O_2 molecule in the ORR. Experimentally, there are two main methods used to calculate n for the ORR processed on the basis of the forced convection methods on a RRDE or a rotating disk electrode (RDE). In the RRDE method, the ORR is conducted on the disk electrode and the production of H_2O_2 can be directly measured by oxidizing it on the ring via



Received: June 5, 2016

Published: June 9, 2016

The n_{RRDE} value can be calculated from the disk current (i_d) and ring current (i_r) using eq 1:

$$n = 4 \times \frac{i_d}{i_d + \frac{i_r}{N_C}} \quad (1)$$

where N_C is the collection efficiency of the RRDE, defined as the fraction of product from the disk to the ring. Analogously, the H_2O_2 ratio (p) is defined as the fraction of O_2 reduced to H_2O_2 and is calculated by eq 2:

$$p = 2 \times \frac{\frac{i_r}{N_C}}{i_d + \frac{i_r}{N_C}} \quad (2)$$

The derivation of eqs 1 and 2 is provided in the Supporting Information. Obviously, n and p relate to each other as follows:

$$n = 4 - 2p \quad (3)$$

Another method is based on the KL theory, specifically on eq 4, which describes the current density behavior on RDE.²⁴

$$\frac{1}{j} = \frac{1}{j_K} + \frac{1}{j_L} = \frac{1}{B} \omega^{-1/2} + \frac{1}{j_K} \quad (4)$$

where j , j_K , and j_L are the measured, kinetic-limited, and mass-transfer-limited current densities, respectively. j_K is assumed to be a constant at a certain potential. j_L is proportional to the square root of angular velocity (ω) of the RDE. The proportionality coefficient (B) is

$$B = 0.62D^{2/3}\nu^{-1/6}nFC^* \quad (5)$$

where D is the diffusion coefficient of the reactant, ν is the kinematic viscosity of the electrolyte, F is the Faraday constant, and C^* is the concentration of the reactant in the bulk electrolyte. Thus, n can be deduced from the slope of the linear plot of j^{-1} versus $\omega^{-1/2}$ (KL plot).

1.3. Brief Review of the History of Calculation of n .

Early ORR studies referred to Pt catalyst in acid electrolytes. Frumkin et al. first used the RRDE to qualitatively detect H_2O_2 produced in the ORR¹⁴ but did not introduce the concept of n or p at that time. The concept of p was introduced by Müller et al.,¹⁵ who measured I_d and I_r at different ω values and got different I_r/I_d values at certain potentials, which means that p is not constant. From the 1960s to the 1980s, the ORR mechanism was studied on the basis of the I_r/I_d vs ω plots and mathematical modeling,^{25–28} without considering n or p values. It was a consensus at that time that I_r/I_d depends on ω ; therefore n and p are not intrinsic properties of a catalyst but are dependent on measurement conditions. Moreover, Damjanovic et al.²⁹ theoretically proved that the ratio between electrochemical reaction rates of direct and indirect pathways plotted against $\omega^{-1/2}$ obeys a linear relationship under the assumption that all the subreactions are first order. Obviously, the ORR has such parallel pathways, i.e. reaction 4e and reactions 2e + 2'e; therefore, I_r/I_d should depend on ω . However, this key fact has been ignored by most researchers since the 1990s. For example, Gasteiger et al. reported different I_r/I_d values at different ω but they did not discuss its origin.^{30,31} In addition, in most recent studies, not much attention was given to the use of proper conditions for performing RRDE experiments. Paulus et al. used the RRDE method to measure n for the first time.³² However, they did not check the H_2O_2

collection reaction on the ring, which must be mass transfer limited to validate the use of the RRDE method.

The KL theory was originally developed to measure physical quantities, such as the diffusion coefficient of a solute, using certain electrochemical reactions (n was considered as a constant). It is difficult to trace the very first report on the KL plot based calculation of n for the ORR, but some papers on this subject started to appear in the 1990s.³³ Since the beginning of the 21st century, most of the ORR-related research has been focused on the development of new catalysts but did not consider the limitations of the KL method. Though there is no evidence in the literature that n is an intrinsic property of the ORR, the KL equation has been often used to calculate n . However, as indicated above, n is not constant during the ORR process measured by the RRDE method.^{24,34} Additionally, the KL method is only valid for one-step reactions, but the ORR is often a multistep process with at least one releasable intermediate. Johnson et al. examined the validity of the KL method in their important review article from the viewpoint of its use for estimation of n for various multistep reactions.³⁵ They concluded that the KL plot is not linear for multistep reactions and the KL plot slope is a function of ω and potential, even if n is a constant. Compton et al. also proved that the KL plot is affected by the coverage of catalysts on the working electrode.³⁶ Therefore, all above evidence indicates that the KL method is not applicable to the evaluation of n for the ORR.

Some problems of this method have been also reviewed recently by Lee et al., who summarized the existing inconsistencies in the literature.³⁷ Some other papers reported experimental observations, including disagreement between the n_{RRDE} and n_{KL} values, but they did not interpret their origin.^{21–23} In our previous papers we also continuously found nonlinear behavior of the KL plots and pointed out the resulting inconsistencies between n_{RRDE} and n_{KL} .^{17–20} In some high-impact papers only the RRDE method was used, probably because the authors noticed the existing inconsistencies.^{13,38–40} However, numerous researchers continue to use the KL method to calculate n . Thus, systematic experimental and theoretical studies are extremely desirable to figure out the problems and develop a correct and accurate method for the determination of n .

On the basis of the aforementioned concerns, here we carefully test both the KL and RRDE methods for several representative catalysts including metals (Au, Ag, and Ru) and carbon-based catalysts (O, N, and Co/N doped graphenes) with planar or 3D structures. A mathematical procedure is proposed to explain the obtained results. The findings include the following.

(i) In the RRDE method, differently to previous studies which adopted the N_C from manufacturers, we found that N_C decreases significantly with catalyst loading. Furthermore, when the electrode surface is rough, N_C also decreases dramatically with ω .

(ii) The widely applied RRDE method with a Pt ring is not suitable for H_2O_2 collection in alkaline electrolytes because the oxidation of H_2O_2 on Pt is not the mass-transfer-limited process. As an alternative, a properly biased Au ring is suitable for H_2O_2 collection and leads to accurate n values.

(iii) The n value significantly depends on ω for all tested catalysts at any potential, which means that the KL method, which requires n to be constant at certain potentials, is not applicable for the ORR. As a result, the calculated n_{KL} values are

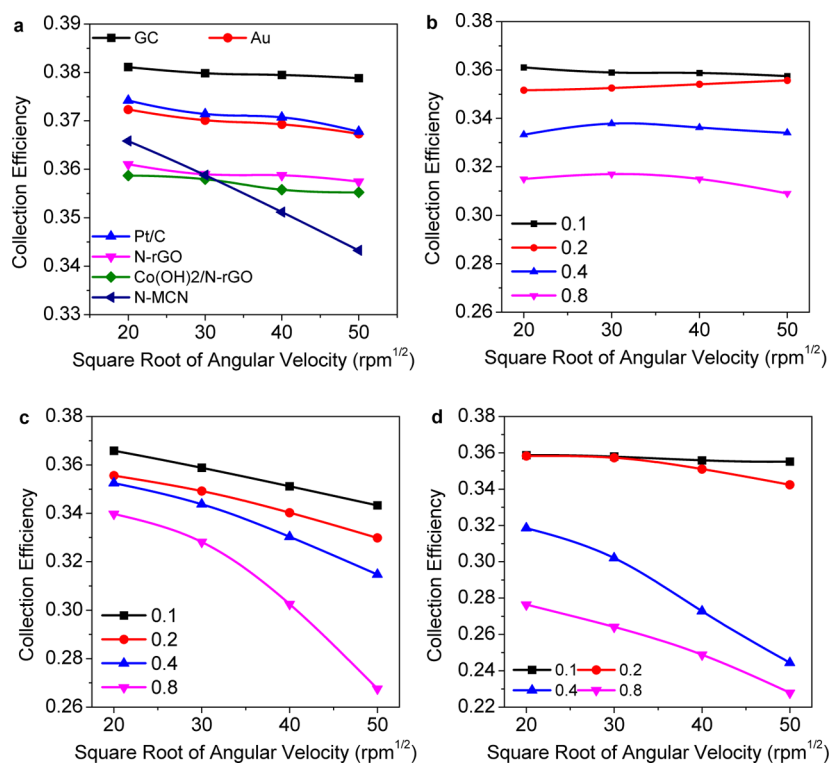


Figure 1. (a) N_C of RRDE loaded with catalysts. The loadings are 0.1 mg cm^{-2} except for Au. (b–d) N_C of RRDE loaded with N-rGO (b), N-MCN (c), and $\text{Co(OH)}_2/\text{N-rGO}$ (d). The values are the loading amounts of catalysts in mg cm^{-2} .

significantly different from the n_{RRDE} values for all tested catalysts at almost any potential.

(iv) Last but not most important, by introducing a simple mathematical procedure, we proved that if all subreactions in the ORR are first order, the value of n depends on ω and the p^{-1} vs $\omega^{-1/2}$ plot is linear, providing a fundamental explanation of the observed phenomena. Also, our results show that the ORR subreactions are not always first order.

These findings prove that only the RRDE method with a properly biased Au ring and calibrated collection efficiency is correct from both theoretical and experimental viewpoints. These conclusions are essential for a proper understanding of the electron transfer number for the ORR processes, allowing an accurate methodology to be established for an accurate determination of n .

2. METHODS

The preparation of catalysts is described in detail in the Supporting Information. The disk diameter, ring inner diameter, and ring outer diameter of the RRDE (AFE7R9GCPT or AFE7R9GCAU, Pine Research Instrument) are 5.61, 6.25, and 7.92 mm, respectively. The N_C value provided by the manufacturer is 0.37. An Ag/AgCl (in 4 M KCl) reference electrode and a Pt-wire counter electrode were used. The calibration of N_C and H_2O_2 oxidation tests are described in the Results and Discussion.

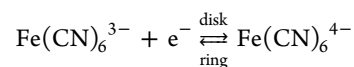
O_2 -saturated 0.1 M KOH was used as the electrolyte unless otherwise specified. The ORR polarization curves were collected using linear scanning voltammetry (LSV) from 1 to 0 V (vs reversible hydrogen electrode, RHE) with a scanning rate of 10 mV s^{-1} . The potential was iR -compensated with electrolyte resistance (30Ω). The currents were subtracted with the background measured in O_2 -free electrolyte (see

Figure S1 in the Supporting Information for details on the electrochemical measurements).

The n_{RRDE} value was calculated by eq 1. The n_{KL} value was calculated by linear fitting (least-squares method) of the KL plot. The parameters used in the KL equation are provided in the Supporting Information.

3. RESULTS AND DISCUSSION

3.1. N_C of RRDE Loaded with Catalysts. Two conditions should be fulfilled before the RRDE method is used. First, N_C should be accurate. Second, the collection reaction on the ring must be limited by mass transfer.²⁴ The N_C value of an ideal RRDE is determined only by its geometry parameters; in other words, it is independent of the reaction and ω . However, when a thick catalyst layer is loaded on the disk, the geometry of the RRDE changes; therefore, it is necessary to calibrate the N_C value of the RRDE with the catalyst. The calibration of N_C is carried out using a simple one-electron transfer redox pair (see the Supporting Information for details).



First, the LSV curves for a glassy-carbon (GC) disk and Pt ring were checked. The results are shown in Figures S3 and S4 in the Supporting Information. When the ring is biased at 1.5 V, I_r is limited by the mass transfer. Thus, the ratio of I_r to I_d is N_C . The N_C values of the RRDE loaded with catalysts are shown in Figure 1a.

The N_C value of our bare RRDE was found to be not 0.37 as supplied by the manufacturer but close to 0.38, probably due to the slight change in the shape after heavy usage. All N_C values loaded with catalysts are lower than the bare value. The reason is that, when the catalyst is loaded on the disk, the electrode–

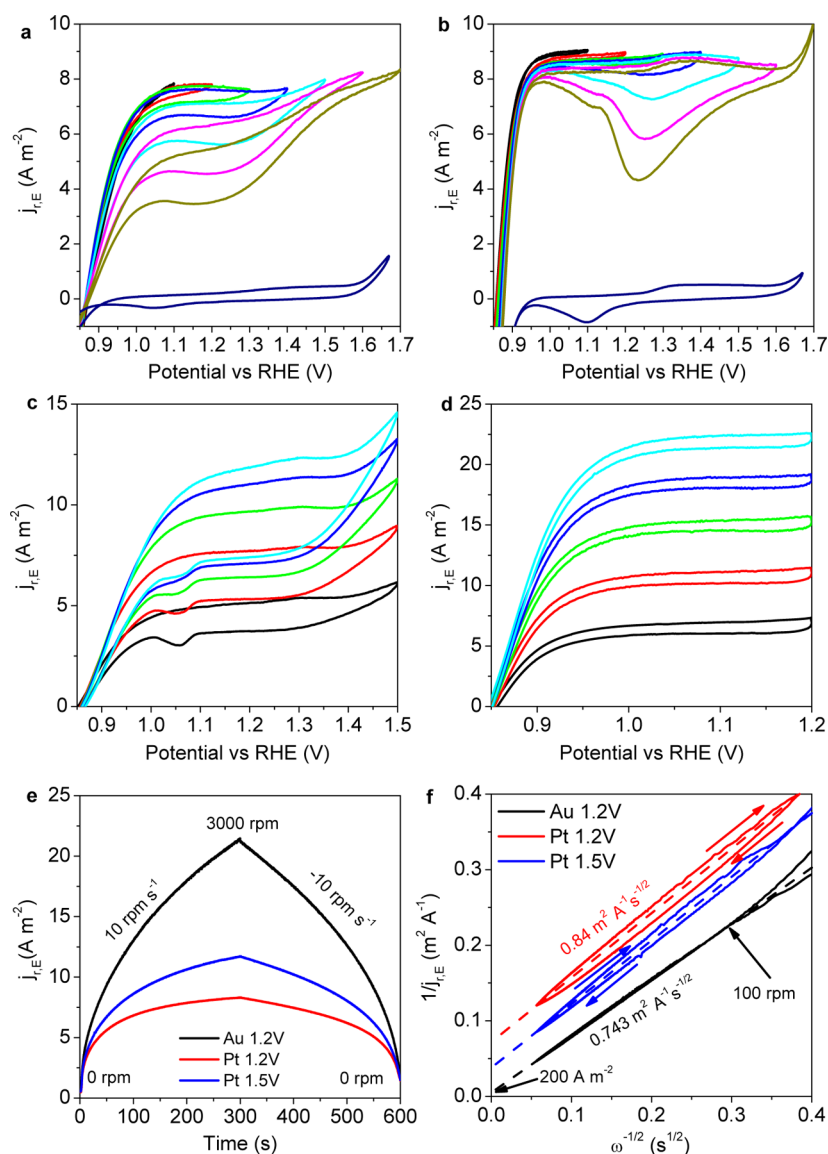


Figure 2. H_2O_2 oxidation experiments in alkaline electrolyte: CVs of Pt ring (a) and Au ring (b) at 400 rpm and CVs of Pt ring (c) and Au ring (d) at ω values of 225, 625, 1225, 2025, and 3025 rpm from bottom to top. The scan rate is 10 mV s^{-1} . (e) Amperometric $i-t$ plots. (f) KL plots derived from (e). The electrolyte is 0.1 M KOH containing 1 mM H_2O_2 for all experiments except the lowest curves in (a) and (b).

electrolyte interface is slightly off the plane of the ring, which decreases the fraction of the product from the catalyst to the ring. Nitrogen doped reduced graphene oxide (N-rGO) and nitrogen doped mesoporous carbon nanospheres (N-MCN) are typical metal-free ORR catalysts; therefore, they are used as examples. As shown in Figure 1b, N_C decreases significantly when N-rGO is loaded. N_C decreases with not only catalyst loading but also ω decreases when N-MCN is loaded (Figure 1c), which is attributed to the turbulence in the electrolyte flow. As shown in Figures S5 and S6 in the Supporting Information, the surface of the N-rGO electrode is much smoother than that of the N-MCN electrode. Turbulence takes place when the fluid flows over a rough surface, which breaks the linearity of the RRDE hydrodynamics and leads to a decrease in N_C . The turbulence degree increases with the roughness of the surface and the speed of the fluid, which is related to ω . The N_C value of RRDE loaded with $\text{Co}(\text{OH})_2/\text{N-rGO}$ decreases dramatically only when the loading of a catalyst is high (Figure 1d) because of the cracking of the catalyst layer (Figure S7 in the

Supporting Information). Such 3D catalysts are well-known for their porous structure and high surface area, which are regarded as reasons for their high ORR performance.⁹ However, the rough catalyst layer actually changes the geometry of the RRDE and introduces significant turbulence; therefore, the measured n may not reflect the real catalytic behavior. A change in the electrode geometry also affects the calculation of n using the KL method (see section 1.7 and Figure S2 in the Supporting Information); therefore, the catalyst layer must be very thin and smooth for accurate measurements if the RDE method and the corresponding hydrodynamic model are used.

3.2. H_2O_2 Oxidation by Pt and Au Rings. It is critical that all of the products from the disk to the ring must participate in the collection reaction; otherwise, I_r/N_C is not the current on the disk. In other words, the collection reaction on the ring must be limited by mass transfer (as in Figure S1 in the Supporting Information). As far as we know, there has been no report on the examination of H_2O_2 oxidation in alkaline

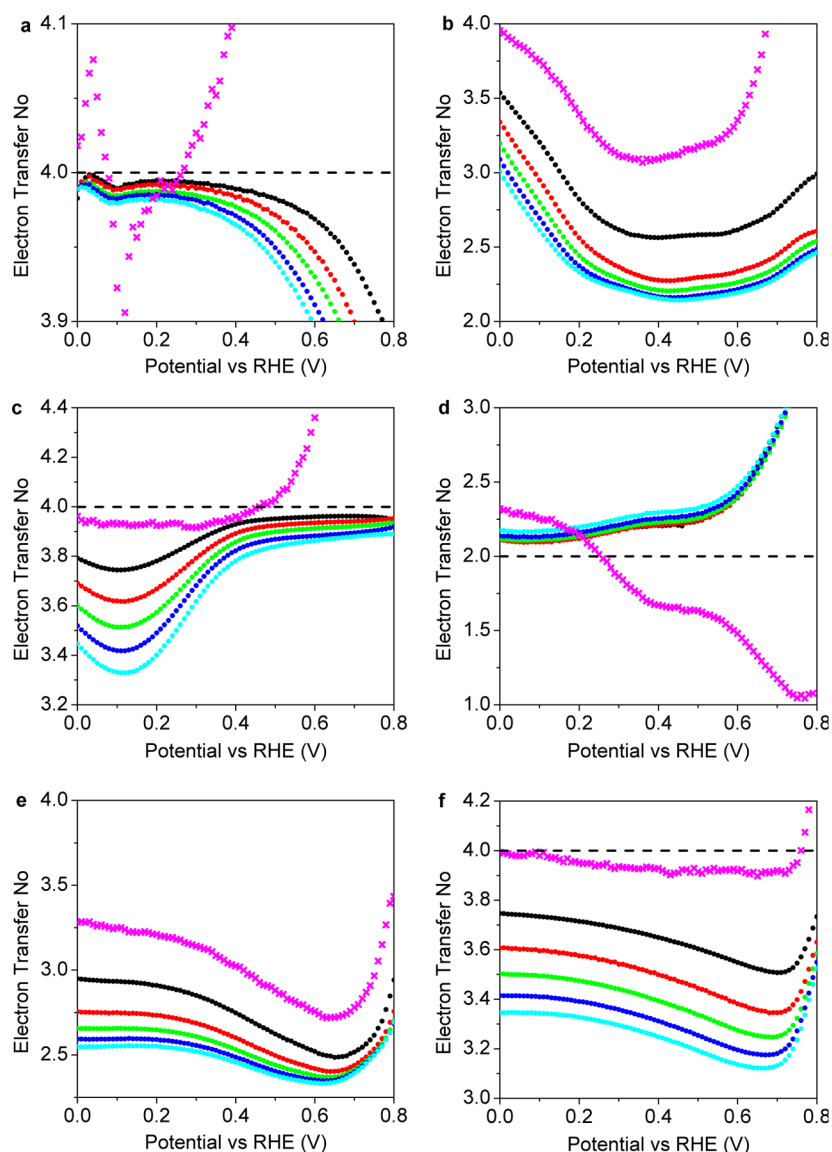


Figure 3. Electron transfer number n estimated for Ru (a), Au (b), Ag (c), e-rGO (d), N-rGO (e) and $\text{Co}(\text{OH})_2/\text{N-rGO}$ (f). n_{RRDE} (circle) values are measured at ω values of 225 rpm (black), 625 rpm (red), 1225 rpm (green), 2025 rpm (blue), and 3025 rpm (cyan). Magenta crosses refer to the n_{KL} values.

electrolyte on a Pt ring. Traditionally, the ring potential is set between 1.2 and 1.5 V, which is expected to be high enough for fast H_2O_2 oxidation but low enough to prevent oxygen evolution. This is examined by the deliberate addition of H_2O_2 to the electrolyte. Figure 2a shows the cyclic voltammetry (CV) curves of the Pt ring. The equivalent ring current density ($j_{r,E}$) is used in the plot because, according to the forced convection hydrodynamic theory,²⁴ the mass-transfer-limited current of a rotating ring electrode is

$$i_{r,L} = B\omega^{1/2}\pi(r_3^3 - r_2^3)^{2/3} \quad (6)$$

where r_2 and r_3 are the inner and outer diameters of the ring. The term $\pi(r_3^3 - r_2^3)^{2/3}$ has exactly the same function as the area. Therefore, $j_{r,E}$ is defined as

$$j_{r,E} = \frac{i_r}{\pi(r_3^3 - r_2^3)^{2/3}} \quad (7)$$

where i_r is the measured ring current.

It is obvious that the CV curve measured on the Pt ring in 0.1 M KOH with 1 mM H_2O_2 does not show a typical mass transfer limitation at any potential. According to previous studies,^{41,42} the rate of electrochemical oxidation of H_2O_2 on Pt is limited by the internal electron transfer from H_2O_2 to oxidized $\text{Pt}(\text{OH})_2$ rather than mass transfer. Figure 2b shows the CV curve measured on an Au ring with the same geometry under the same conditions. The oxidation of the Au surface does not take place below 1.2 V, at which the mass transfer limitation of H_2O_2 oxidation seems to be achieved. The current on Au is also higher than that on Pt at any potential; thus, it proves again that the current on the Pt ring is not limited by mass transfer. Figure 2c,d shows the CV curves on Pt and Au rings, measured at the fixed ranges but different ω values. The conclusions are the same.

To prove the H_2O_2 oxidation on Au ring at 1.2 V is mass transfer limited, the amperometric $i-t$ measurements were performed. This time, the potential was fixed while ω was scanned from 0 to 3000 rpm and back to 0 rpm with 10 rpm

s^{-1} . As shown in Figure 2e, the current on the Au ring at 1.2 V is much higher than that on the Pt ring at 1.2 and 1.5 V. The corresponding KL plots are shown in Figure 2f. On the Au ring, the positive and negative scans overlap very well in the range of 100–3000 rpm, which means that the H_2O_2 oxidation on Au is highly reproducible (without hysteresis). The intercept of the KL plot is about $200 A m^{-2}$, which is at least 5 times higher than the ring currents in ORR (shown later). Therefore, the H_2O_2 oxidation is very close to the mass transfer limitation on the Au ring. In contrast, the KL plots of positive and negative scans of Pt ring do not overlap. The KL plots of the Pt ring are also not linear; the intercepts are far from the origin, and the slopes are larger than that on the Au ring. This proves that the Pt ring current is not mass transfer limited. Therefore, using the Pt ring to collect H_2O_2 can lead to underestimated p values or overestimated n values. The Au ring biased at 1.2 V is suitable for H_2O_2 collection in alkaline electrolyte. All of the ORR results shown below were obtained by using RRDE with an Au ring.

The H_2O_2 oxidation was also measured in acidic electrolyte (0.05 M H_2SO_4 , 1 Mm H_2O_2). The results are shown in Figures S8 and S9 in the Supporting Information. The H_2O_2 oxidation on Pt is similar to that in alkaline electrolyte. The oxidation of the Pt surface has a strong effect on the H_2O_2 oxidation activity, and the current never reaches the mass transfer limitation at any potential below oxygen evolution. Since both the alkaline and acidic electrolytes used were dilute solutions, their viscosities as well as the diffusion coefficients of H_2O_2 in these solutions should be very similar; therefore, the mass transfer limiting currents should be similar as well. Thus, by a comparison of the maximum currents in alkaline and acidic electrolytes, it is easy to find that the H_2O_2 oxidation in acidic electrolytes is far from completion; thus, n cannot be measured accurately in the latter electrolytes with the Pt ring. On the Au ring, the H_2O_2 oxidation current is even lower than that on Pt. Since we have not found a proper ring material to measure H_2O_2 accurately in acidic electrolyte, the results and discussion of n are all based on data in alkaline electrolyte.

3.3. Measured Electron Transfer Number. Three typical non-Pt-group metals (Ru, Au, and Ag) and three typical carbon-based catalysts were tested. Among the carbon-based catalysts, electrochemically reduced graphene oxide (e-rGO) can be viewed as a typical oxygen-doped carbon. N-rGO is a typical nitrogen-doped carbon. $Co(OH)_2/N-rGO$ is a typical non-precious-metal catalyst with metal–nitrogen–carbon structure. All carbon catalysts have a loading of $0.1 mg cm^{-2}$ so that N_C is almost constant (0.37) at any ω . The RRDE polarization curves are provided in Figures S10–S21 in the Supporting Information. The ring current densities are normalized to the disk area and divided by N_C . The n_{KL} values are calculated on the basis of j_d at all ω . The KL plots at selected potentials are provided in Figures S22–S27 in the Supporting Information. The n_{RRDE} and n_{KL} values obtained for the catalysts studied are shown in Figure 3.

As the calculated n_{KL} also depends on the parameters in eq 5, Ru is used as a benchmark to calibrate them. The n_{RRDE} value of Ru is very close to 4 at 0.2 V (Figure 3a). At this potential, the ORR process on Ru is also mass transfer limited (Figure S8 in the Supporting Information). Therefore, j is equal to j_L and n is 4 in eq 5. By using the proper parameters (see the Supporting Information), the n_{KL} value at 0.2 V is set to 4. These parameters are used in all subsequent n_{KL} calculations. On Ru below 0.2 V, the underpotential deposition of hydrogen occurs

so that n_{KL} is affected. Above 0.2 V, n_{RRDE} decreases with potential at any ω . A significant change of n_{RRDE} with ω is also observed. In contrast, the calculated n_{KL} increases as the potential increases from 0.2 V, which exceeds the theoretical limitation of 4, and even goes to an unreasonably high value at higher potential; thus, it must be incorrect. The trends of n on Au, Ag, N-rGO, and $Co(OH)_2/N-rGO$ are similar to those on Ru, on which the n_{RRDE} decreases as ω increases, the n_{KL} values are higher than the corresponding n_{RRDE} values, and the n_{KL} values go to infinity at high potential. The only exception is e-rGO, on which n_{RRDE} increases as ω increases and the corresponding n_{KL} is mostly lower than n_{RRDE} and reaches a value smaller than 2 (another theoretical limitation) at high potential.

The relationship between n_{KL} and real n on all catalysts except e-rGO can be qualitatively explained on the basis of the calculation process of n_{KL} . When the KL equation is used, j_L is assumed proportional to $\omega^{1/2}$, but it actually increases more slowly than is assumed because of a decrease of n ; therefore, the KL slope is lower than it should be. The lower KL slope leads to higher calculated values of n_{KL} . The trend is just reversed on the e-rGO catalyst, for which n increases as ω increases. Therefore, the change of n with ω makes the KL method incorrect on all catalysts.

3.4. Mathematical Modeling. To figure out the existing problems of the KL method and explain the n_{RRDE} , the derivation of the hydrodynamic model has been carefully examined. A simple solution of the convective-diffusion equation for a one-step and one-way reaction is provided in Bard's textbook.²⁴ Note that the term "one-way" reaction is used when the reverse reaction does not occur under particular conditions (electrode potentials) so that the KL method can be employed; it cannot be confused with the term "irreversible", which usually refers to the situation when the reverse reaction never takes place. The result is represented by

$$\frac{j}{nF} = m(C^* - C^0) \quad (8)$$

where j is the current density, C^0 is the concentration of reactant on the electrode surface, and m is the mass transfer coefficient of the reactant, which is given by

$$m = 0.62D^{2/3}\nu^{-1/6}\omega^{1/2} \quad (9)$$

The physical meaning of eq 8 is that the current density is proportional to the flux of reactant. If the reaction is first-order, the current density is proportional to C^0 :

$$j = nkFC^0 \quad (10)$$

where k is the reaction rate constant. Combining eqs 8 and 10 yields

$$\frac{1}{j} = \frac{1}{nFmC^*} + \frac{1}{nkFC^*} \quad (11)$$

where $nFmC^*$ is the current density limited by mass transfer, which is denoted by j_L (Levich theory). $nkFC^*$ is the current density limited by reaction kinetics (in absence of mass transfer effects), which is denoted by j_K (Koutecky theory). Then eq 10 can be rewritten as eq 4. Note that this result is based on the assumption of a one-step, one-way, and first-order reaction. Often, the ORR process is not a one-step reaction, as indicated in the Introduction. Furthermore, the equilibrium potential of reaction 2e is about 0.7 V, which is within the ORR potential

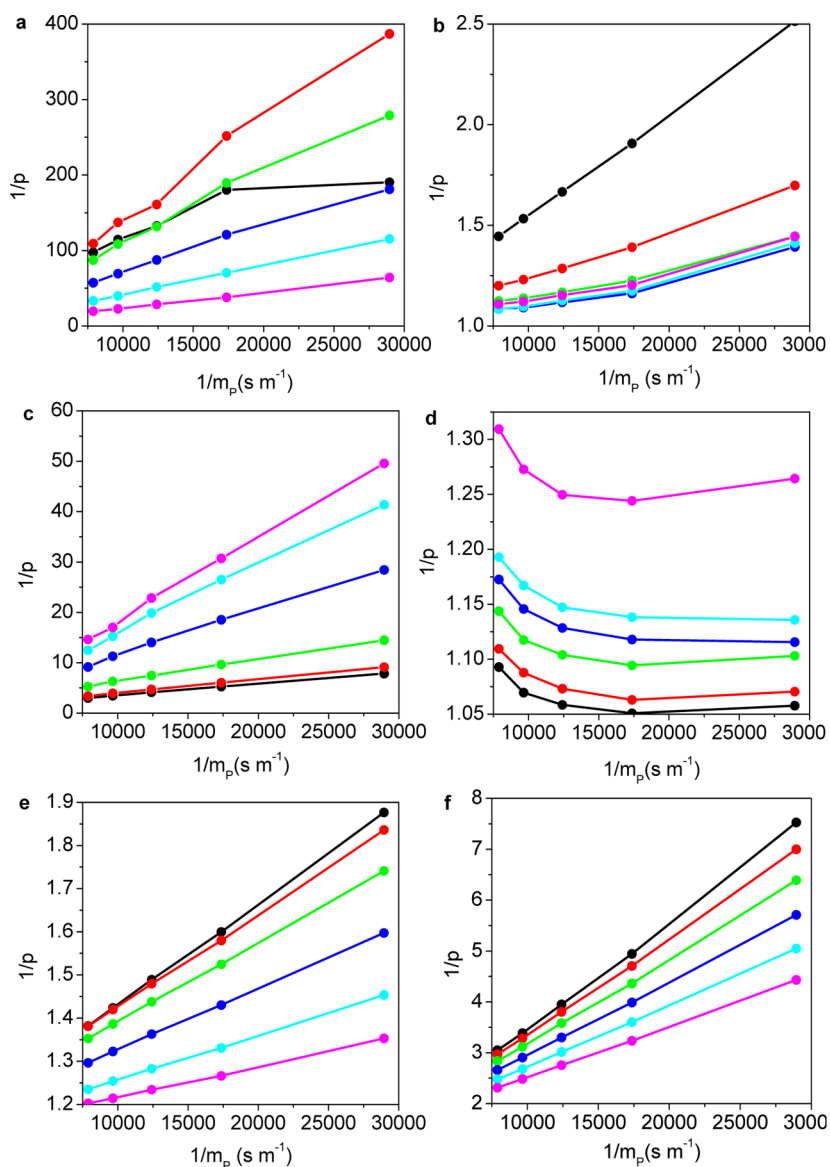


Figure 4. $1/p$ vs $1/m_p$ plots for ORR on Ru (a), Au (b), Ag (c), e-rGO (d), N-rGO (e), and Co(OH)₂/N-rGO (f). The potentials are 0.1 V (black), 0.2 V (red), 0.3 V (green), 0.4 V (blue), 0.5 V (cyan), and 0.6 V (magenta), respectively.

window (0 to 1 V), so reaction 2e represents a two-way reaction around a potential of 0.7 V. Therefore, the conditions of the KL theory are not satisfied by the ORR. A revised form of the equations can be derived for the ORR, which takes into account the multistep nature of ORR but retains the first-order assumption, as shown below.

In ORR, there are two reactants: O₂ and H₂O₂. Their corresponding parameters (C , m , and D) are subscripted by O and P, respectively. The current densities and rate constants of reactions 4e, 2e and 2'e are subscripted by 4, 2, and -2 (reverse reaction) and 2', respectively. According to the solution of the convective-diffusion equation, the following equations can be constructed, which are similar to eq 8:

$$\frac{j_4}{4F} + \frac{j_2}{2F} = m_O(C^*_O - C^0_O) \quad (13)$$

$$\frac{j_{2'}}{2F} - \frac{j_2}{2F} = m_P(C^*_P - C^0_P) \quad (14)$$

The physical meaning of eqs 13 and 14 is that the current densities of O₂- and H₂O₂-related reactions are proportional to their fluxes. C^*_P is 0 because H₂O₂ is not present in the bulk electrolyte. Assuming all subreactions are first order, similar to eq 10, the current densities of the subreactions can be presented as

$$j_4 = 4Fk_4C^0_O \quad (15)$$

$$j_{2'} = 2Fk_2C^0_P \quad (16)$$

$$j_2 = 2Fk_2C^0_O - 2Fk_{-2}C^0_P \quad (17)$$

Here, we have five unknowns, j_2 , j_4 , $j_{2'}$, C^0_O , and C^0_P , and five linear equations: eqs 13–17. Therefore, all of the unknowns can be solved. The complete set of solutions is

$$C^0_P = \frac{k_2 m_O C^*_O}{(k_4 + k_2 + m_O)(k_{-2} + k_{2'} + m_P) - k_2 k_{-2}} \quad (18)$$

$$C_{\text{O}}^0 = \frac{m_{\text{O}} C_{\text{O}}^* (k_{-2} + k_{2'} + m_{\text{p}})}{(k_4 + k_2 + m_{\text{O}})(k_{-2} + k_{2'} + m_{\text{p}}) - k_2 k_{-2}} \quad (19)$$

$$j_4 = \frac{4Fk_4 m_{\text{O}} C_{\text{O}}^* (k_{-2} + k_{2'} + m_{\text{p}})}{(k_4 + k_2 + m_{\text{O}})(k_{-2} + k_{2'} + m_{\text{p}}) - k_2 k_{-2}} \quad (20)$$

$$j_{2'} = \frac{2Fk_2 k_2' m_{\text{O}} C_{\text{O}}^*}{(k_4 + k_2 + m_{\text{O}})(k_{-2} + k_{2'} + m_{\text{p}}) - k_2 k_{-2}} \quad (21)$$

$$j_2 = \frac{2Fk_2 m_{\text{O}} C_{\text{O}}^* (k_{2'} + m_{\text{p}})}{(k_4 + k_2 + m_{\text{O}})(k_{-2} + k_{2'} + m_{\text{p}}) - k_2 k_{-2}} \quad (22)$$

The disk current is the sum of j_4 , $j_{2'}$, and j_2 , which is

$$j_{\text{d}} = 2Fm_{\text{O}} C_{\text{O}}^* \frac{2k_4(k_{-2} + k_{2'} + m_{\text{p}}) + 2k_2 k_2' + k_2 m_{\text{p}}}{(k_4 + k_2 + m_{\text{O}})(k_{-2} + k_{2'} + m_{\text{p}}) - k_2 k_{-2}} \quad (23)$$

Obviously, j_{d} is no longer in the form of KL eq 4. Therefore, no linear relationship between j_{d}^{-1} and $\omega^{-1/2}$ is expected. The ring current is proportional to the rate of net H_2O_2 production normalized by disk area:

$$\frac{j_{\text{r}}}{N_{\text{C}}} = j_2 - j_{2'} \\ = \frac{2Fm_{\text{p}} m_{\text{O}} C_{\text{O}}^* k_2}{(k_4 + k_2 + m_{\text{O}})(k_{-2} + k_{2'} + m_{\text{p}}) - k_2 k_{-2}} \quad (24)$$

Note that the ratio between j_{r} and j_{d} is not constant at certain rate constants. It is a function of m_{O} and m_{p} , which are functions of ω . These results theoretically prove that the n is a function of ω and the KL method is not correct for the ORR. Inserting eqs 23 and 24 into eq 2 yields

$$p = \frac{m_{\text{p}} k_2}{(k_4 + k_2)(k_{-2} + k_{2'} + m_{\text{p}}) - k_2 k_{-2}} \quad (25)$$

or

$$\frac{1}{p} = \left[\frac{k_4}{k_2} k_{-2} + k_{2'} \left(\frac{k_4}{k_2} + 1 \right) \right] \frac{1}{m_{\text{p}}} + \left(\frac{k_4}{k_2} + 1 \right) \quad (26)$$

This result shows that $1/p$ depends linearly on $1/m_{\text{p}}$. $1/p$ is independent of ω if and only if both $k_{2'}$ and k_{-2} are 0, because k_4/k_2 is always positive. This suggests that the dependence of p on ω originates from reactions 2'e and 2e, in which H_2O_2 is the reactant. To understand this dependence, divide eq 18 by eq 19:

$$\frac{C_{\text{p}}^0}{C_{\text{O}}^0} = \frac{k_2}{k_{-2} + k_{2'} + m_{\text{p}}} \quad (27)$$

Equation 27 shows that the increase of C_{p}^0 with ω is slower than that of C_{O}^0 . The reason is that higher ω accelerates not only the O_2 transfer to the electrode but also the H_2O_2 transfer away from the electrode. Therefore, the increase of reaction 2e with ω is faster than that of reactions 2'e and 2e''; thus, p increases with ω .

The $1/p$ vs $1/m_{\text{p}}$ plot can be used as the criterion of the applicability of our model. If the model is correct, the plot must be linear, the slope must be positive, and the intercept must be larger than 1. The $1/p$ vs $1/m_{\text{p}}$ plots for the all tested catalysts are shown in Figure 4. Obviously, the linearity of $1/p$ vs $1/m_{\text{p}}$ is

not perfectly good for all catalysts due to experimental errors but is quite good in the case of Au, Ag, N-rGO, and $\text{Co}(\text{OH})_2/\text{N-rGO}$. In the case of the Ru electrode, the p value is too close to 0 so that the effects of underpotential deposition of hydrogen are significant. Only the plots obtained for e-rGO violate our model significantly. A possible reason is that both $k_{2'}$ and k_{-2} are almost 0 on e-rGO; therefore, the actual p is very close to 2 and the dependence on ω is very small. On the other hand, the turbulence, which hinders H_2O_2 detection, makes the measured value of p lower at higher ω . As a result, the $1/p$ vs $1/m_{\text{p}}$ plot deviates from our model. In other words, the proposed model can be adopted on the catalysts which activate H_2O_2 consumption. Nevertheless, the principle of dependence of n on the angular velocity will remain the same, even if n cannot be measured accurately as in the case of rough electrodes.

There is still one minor problem: in the case of Au, p seems to increase with ω slightly faster than that predicted by the model, which cannot be explained by turbulence. To explain this phenomenon, one should note that there are two independent groups of processes in the ORR: those occurring within the catalyst layer (reactions and mass transfer in the pores) and those in the electrolyte (forced convection). Therefore, the aforementioned question becomes (1) whether the process within the catalyst layer can be described by rate constants and (2) whether the process in the electrolyte can be described by mass transfer coefficients. It was proved by experiments that the answer to question 2 is positive, if the thickness and roughness of the catalyst do not change the hydrodynamic model significantly. As regards question 1, our results indicate that the reaction rate–concentration relationship can be described by first-order reactions quite accurately on some catalysts. The reason why the ORR on Au is not exact first order is as yet unclear. One reasonable explanation is that the change in the coverage of reactant alters the electrochemical behavior of the catalysts, which affects the apparent order of the reaction. In fact, an electrochemical reaction does not need to be first order. For example, the order of the simplest hydrogen evolution reaction depends on both catalyst and coverage (potential).⁴³ The ORR is much more complicated. And there is already a longstanding controversy on the order of the ORR on Pt.^{44–46} On Au, the adsorption energy of O decreases with increasing coverage according to the theoretical calculations,⁴⁷ and this energy is the main barrier for the ORR on Au; thus, the order of ORR on Au could be higher than 1.

4. CONCLUSIONS

The extensive measurements of electron transfer numbers for the ORR on different electrodes have been examined from experimental and theoretical viewpoints. In reference to the RRDE method, we found that the collection coefficient depends significantly on the loading amount and the surface roughness of a given catalyst. To get accurate results, the loading amount of catalysts should be low and the collection coefficient must be calibrated for each measurement. The Pt ring is proved to be unsuitable for H_2O_2 collection experiments in alkaline electrolyte. Alternatively, the Au ring biased at 1.2 V guarantees that the collection coefficient is valid for H_2O_2 oxidation. We also found that the electron transfer number is dependent on the angular velocity, and the KL method provides results greatly different from those obtained by the RRDE method. By establishing a new mathematical model, we found that the KL method is not suitable for determining the electron transfer number of ORR, since the ORR is neither one

step nor one way. Only the RRDE method with calibrated N_C and a properly biased Au ring is reliable from both theoretical and experimental viewpoints. We further found that the ORR is not always first order. This study provides some recommendations for correct assessment of the performance and mechanism of the ORR processes in alkaline electrolytes.

■ ASSOCIATED CONTENT

■ Supporting Information

The Supporting Information is available free of charge on the ACS Publications website at DOI: 10.1021/acscatal.6b01581.

Synthesis of materials, details of electrochemical experiments, error analysis, SEM images of the samples studied, and LSV and KL plots obtained for the ORR on different electrodes (PDF)

■ AUTHOR INFORMATION

Corresponding Author

*E-mail for S.-Z.Q.: s.qiao@adelaide.edu.au.

Present Address

^{||}Graduate School of Chemical Sciences and Engineering, Hokkaido University, Sapporo, Hokkaido 060-0810, Japan.

Notes

The authors declare no competing financial interest.

■ ACKNOWLEDGMENTS

We especially thank Prof. Piotr Zelenay of Los Alamos National Laboratory for his kind comments and suggestions on this work. This work has been financially supported by the Australian Research Council (ARC) through Discovery Project programs (DP130104459, DP140104062, and DP 160104866).

■ REFERENCES

- (1) Jirkovsky, J. S.; Panas, I.; Ahlberg, E.; Halasa, M.; Romani, S.; Schiffrin, D. J. *J. Am. Chem. Soc.* **2011**, *133*, 19432–19441.
- (2) Assumpcao, M.; De Souza, R. F. B.; Rascio, D. C.; Silva, J. C. M.; Calegari, M. L.; Gaubeur, I.; Paixao, T.; Hammer, P.; Lanza, M. R. V.; Santos, M. C. *Carbon* **2011**, *49*, 2842–2851.
- (3) Fu, L.; You, S. J.; Yang, F. L.; Gao, M. M.; Fang, X. H.; Zhang, G. Q. *J. Chem. Technol. Biotechnol.* **2010**, *85*, 715–719.
- (4) Siahrostami, S.; Verdaguier-Casadevall, A.; Karamad, M.; Deiana, D.; Malacrida, P.; Wickman, B.; Escudero-Escribano, M.; Paoli, E. A.; Frydendal, R.; Hansen, T. W.; Chorkendorff, I.; Stephens, I. E. L.; Rossmeisl, J. *Nat. Mater.* **2013**, *12*, 1137–1143.
- (5) Li, H.; Tsay, K.; Wang, H. J.; Shen, J.; Wu, S. H.; Zhang, J. J.; Jia, N. Y.; Wessel, S.; Abouatallah, R.; Joos, N.; Schrooten, J. *J. Power Sources* **2010**, *195*, 8089–8093.
- (6) Qiao, J. L.; Saito, M.; Hayamizu, K.; Okada, T. *J. Electrochem. Soc.* **2006**, *153*, A967–A974.
- (7) Yu, J. R.; Yi, B. L.; Xing, D. M.; Liu, F. Q.; Shao, Z. G.; Fu, Y. Z. *Phys. Chem. Chem. Phys.* **2003**, *5*, 611–615.
- (8) Liang, Y. Y.; Wang, H. L.; Zhou, J. G.; Li, Y. G.; Wang, J.; Regier, T.; Dai, H. J. *J. Am. Chem. Soc.* **2012**, *134*, 3517–3523.
- (9) Wu, Z. S.; Yang, S. B.; Sun, Y.; Parvez, K.; Feng, X. L.; Mullen, K. *J. Am. Chem. Soc.* **2012**, *134*, 9082–9085.
- (10) Liang, Y. Y.; Li, Y. G.; Wang, H. L.; Zhou, J. G.; Wang, J.; Regier, T.; Dai, H. J. *Nat. Mater.* **2011**, *10*, 780–786.
- (11) Li, Y. G.; Zhou, W.; Wang, H. L.; Xie, L. M.; Liang, Y. Y.; Wei, F.; Idrobo, J. C.; Pennycook, S. J.; Dai, H. J. *Nat. Nanotechnol.* **2012**, *7*, 394–400.
- (12) Gong, K. P.; Du, F.; Xia, Z. H.; Durstock, M.; Dai, L. M. *Science* **2009**, *323*, 760–764.
- (13) Wu, G.; More, K. L.; Johnston, C. M.; Zelenay, P. *Science* **2011**, *332*, 443–447.

- (14) Frumkin, A.; Nekrasov, L.; Levich, B.; Ivanov, J. *J. Electroanal. Chem.* **1959**, *1*, 84–90.
- (15) Müller, L.; Nekrasov, L. *Electrochim. Acta* **1964**, *9*, 1015–1023.
- (16) Koutecky, J.; Levich, B. G. *Zh. Fiz. Khim.* **1958**, *32*, 1565–1575.
- (17) Zhou, R. F.; Zheng, Y.; Hulicova-Jurcakova, D.; Qiao, S. Z. *J. Mater. Chem. A* **2013**, *1*, 13179–13185.
- (18) Zhou, R. F.; Qiao, S. Z. *Chem. Mater.* **2014**, *26*, 5868–5873.
- (19) Duan, J. J.; Zheng, Y.; Chen, S.; Tang, Y. H.; Jaroniec, M.; Qiao, S. Z. *Chem. Commun.* **2013**, *49*, 7705–7707.
- (20) Zheng, Y.; Jiao, Y.; Ge, L.; Jaroniec, M.; Qiao, S. Z. *Angew. Chem., Int. Ed.* **2013**, *52*, 3110–3116.
- (21) Kim, J.-D.; Pyun, S.-I.; Yang, T.-H.; Ju, J.-B. *J. Electroanal. Chem.* **1995**, *383*, 161–166.
- (22) Mamlouk, M.; Kumar, S. M. S.; Gouerec, P.; Scott, K. J. *Power Sources* **2011**, *196*, 7594–7600.
- (23) Zhang, H.-J.; Li, H.; Li, X.; Qiu, H.; Yuan, X.; Zhao, B.; Ma, Z.-F.; Yang, J. *Int. J. Hydrogen Energy* **2014**, *39*, 267–276.
- (24) Bard, A. J.; Faulkner, L. R. *Electrochemical Methods: Fundamentals and Applications*; Wiley: New York, 2000.
- (25) Wroblowa, H. S.; Yen Chi, P.; Razumney, G. J. *Electroanal. Chem. Interfacial Electrochem.* **1976**, *69*, 195–201.
- (26) Hsueh, K. L.; Chin, D. T.; Srinivasan, S. *J. Electroanal. Chem. Interfacial Electrochem.* **1983**, *153*, 79–95.
- (27) Anastasijevic, N. A.; Vesovic, V.; Adzic, R. R. *J. Electroanal. Chem. Interfacial Electrochem.* **1987**, *229*, 305–316.
- (28) Anastasijevic, N. A.; Vesovic, V.; Adzic, R. R. *J. Electroanal. Chem. Interfacial Electrochem.* **1987**, *229*, 317–325.
- (29) Damjanovic, A.; Genshaw, M. A.; Bockris, J. O.; apos, M. J. *Chem. Phys.* **1966**, *45*, 4057–4059.
- (30) Gasteiger, H. A.; Ross, P. N. *J. Phys. Chem.* **1996**, *100*, 6715–6721.
- (31) Markovic, N. M.; Gasteiger, H. A.; Ross, P. N. *J. Phys. Chem.* **1995**, *99*, 3411–3415.
- (32) Paulus, U. A.; Schmidt, T. J.; Gasteiger, H. A.; Behm, R. J. *J. Electroanal. Chem.* **2001**, *495*, 134–145.
- (33) El Mouahid, O.; Coutanceau, C.; Belgsir, E. M.; Crouigneau, P.; Léger, J. M.; Lamy, C. *J. Electroanal. Chem.* **1997**, *426*, 117–123.
- (34) Pleskov, I. U. V.; Filinovski, V. I. U. *The rotating disc electrode*; Consultants Bureau: New York, 1976.
- (35) Treimer, S.; Tang, A.; Johnson, D. C. *Electroanalysis* **2002**, *14*, 165–171.
- (36) Masa, J.; Batchelor-McAuley, C.; Schuhmann, W.; Compton, R. *Nano Res.* **2014**, *7*, 71–78.
- (37) Shin, D.; Jeong, B.; Choun, M.; Ocon, J. D.; Lee, J. *RSC Adv.* **2015**, *5*, 1571–1580.
- (38) Zhou, R.; Qiao, S. Z. *Chem. Commun.* **2015**, *51*, 7516–7519.
- (39) Wu, G.; More, K. L.; Xu, P.; Wang, H. L.; Ferrandon, M.; Kropf, A. J.; Myers, D. J.; Ma, S. G.; Johnston, C. M.; Zelenay, P. *Chem. Commun.* **2013**, *49*, 3291–3293.
- (40) Chung, H. T.; Won, J. H.; Zelenay, P. *Nat. Commun.* **2013**, *4*, 1922.
- (41) Hall, S. B.; Khudaish, E. A.; Hart, A. L. *Electrochim. Acta* **1998**, *43*, 579–588.
- (42) Hall, S. B.; Khudaish, E. A.; Hart, A. L. *Electrochim. Acta* **1998**, *43*, 2015–2024.
- (43) Conway, B. E.; Salomon, M. *Electrochim. Acta* **1964**, *9*, 1599–1615.
- (44) Ross, P. N.; Andricacos, P. C. *J. Electroanal. Chem. Interfacial Electrochem.* **1983**, *154*, 205–215.
- (45) Ross, P. N.; Cairns, E. J.; Striebel, K.; McLarnon, F.; Andricacos, P. C. *Electrochim. Acta* **1987**, *32*, 355–355.
- (46) Hsueh, K. L.; Chang, H. H.; Chin, D. T.; Srinivasan, S. *Electrochim. Acta* **1985**, *30*, 1137–1142.
- (47) Shi, H.; Stampfl, C. *Phys. Rev. B: Condens. Matter Mater. Phys.* **2007**, *76*, 075327.